16th World Conference on Earthquake, 16WCEE 2017
Santiago Chile, January 9th to 13th 2017
Paper N° 524
Registration Code: S-R1461896743

STUDY ON A NEW TYPE OF EARTHQUAKE RESILIENT SHEAR WALL

Q.Z. Liu[(1)], H.J. Jiang[(2)]

[(1)] PhD Candidate, State Key Laboratory of Disaster Reduction in Civil Engineering, Tongji University, Shanghai 200092, China, 384548027@qq.com
[(2)] Professor, State Key Laboratory of Disaster Reduction in Civil Engineering, Tongji University, Shanghai 200092, China, jhj73@tongji.edu.cn

Abstract

RC shear walls have been widely used in tall buildings in earthquake prone areas around the world due to their high lateral stiffness and strength. It has been found from the past earthquake that RC shear walls easily suffer severe damage concentrating at the bottom. In this study a new type of earthquake resilient RC shear wall with the new replaceable energy-dissipation components installed at the two bottom corner of the wall was proposed. The replaceable component is mainly composed of the buckling-restrained mild steel core and the concrete filled steel tube. During the strong earthquake the damage is expected to concentrate at the replaceable components rather than the other part of the wall so that the shear wall can be easily repaired and the building can restore its function quickly after the earthquake. The quasi-static tests under cyclic loading were carried out on one traditional RC shear wall specimen and two new shear wall specimens with the aspect ratio of 3.2 and the axial compressive load ratio of 0.25 due to the limitation of loading capacity. The test results show that the new shear wall specimen installed with the replaceable components has much higher carrying capacity, ductility, and energy-dissipation capacity, and a little bit higher lateral stiffness than the traditional shear wall specimen. For the two new shear wall specimens, the one with larger cross-sectional area of replaceable components has a little bit higher carrying capacity, lower ductility, and larger energy-dissipation capacity. Compared with the traditional shear wall specimen, the lateral force-top displacement hysteretic behavior of new shear wall specimens is more stable, with less strength and stiffness degradation after the peak load. As expected, although the damage behavior of all the specimens is flexure-dominating, for the new shear wall specimens the damage mainly concentrates at the replaceable components while the left part is well protected, and for the traditional shear wall specimen the damage concentrates at the bottom. Compared with the earthquake resilient shear wall installed with replaceable rubber bearings developed in the literature, the new shear wall proposed in this study has larger lateral strength and stiffness, and the remaining part excluding the replaceable components is better protected when subjected to the strong earthquake. The numerical models for all the specimens were constructed by using the commercial software ABAQUAS. The pushover analyses were conducted. The computational results agree well with the test results. Finally, by using the verified numerical models the seismic behavior of the specimens with higher axial compressive load ratio which matches the real case more in tall buildings was investigated in order to overcome deficiency of the experimental study due to the loading condition limitation. The simulation results show that in the case under higher compressive loading the seismic performance of the new shear wall is improved similarly with the carrying capacity and deformation capacity much higher than that of the traditional shear wall.

Keywords: RC shear wall; earthquake resilient structure; replaceable component; static test; computation simulation

1. Introduction

Earthquakes cause not only the direct economic loss from the damage of the structural components and non-structural components, but also the indirect economic loss from the temporary suspension of living and production. The economic loss will be reduced significantly if the structure can retain or restore its function rapidly after the earthquake. The earthquake resilient structure is the structure which can restore immediately the structural function after an earthquake without significant retrofit. Up to now, there are mainly three types of earthquake resilient structures developed by the researchers, i.e., the rocking structures [1, 2], the self-centering structures [3, 4], and the structures with replaceable structural components [5, 6].

Reinforced concrete (RC) shear walls have been widely used in tall buildings in earthquake prone areas due to their high lateral stiffness and strength. It has been found from the past earthquake experience that the RC shear walls in some tall buildings suffered severe damage that concentrated at the bottom, including the crushing and spalling of the concrete, and the buckling or fracture of the longitudinal reinforcement. These kinds of damage are generally very difficult to be repaired, and the cost of repair is very high. To reduce the seismic damage of the shear walls, several types of rocking and self-centering shear wall structures were proposed and implemented in real buildings [7-10]. In addition, the concept of replaceable component was applied in coupling beams of shear wall structures [11, 12].

The new shear wall with the replaceable energy-dissipation components installed at the two bottom corners was proposed by Lu et al. [13]. The improved seismic performance of the new shear wall was verified by the tests. However, from the tests it was found that compared with the normal RC shear wall the lateral stiffness of the new shear wall decreases and the hysteretic behavior of the replaceable component is not very stable. The seismic performance of the new shear wall could be better if the performance of the replaceable component is improved.

In this study, a new kind of replaceable component installed at the two bottom corners of RC shear walls was put forward. Compared with the previous replaceable corner component, the stiffness and energy-dissipation capacity of the new replaceable corner component are much higher. In addition, the construction details of the new shear wall is improved so that the replaceable component can be replaced more conveniently after the strong earthquake and the remaining part can be better protected. The tests on RC shear walls installed with the replaceable components were carried out under cyclic loading to verify its performance. The static pushover analysis using commercial software ABAQUAS was carried out for the new shear wall and the traditional RC shear wall. The numerical model was verified by the test results. Finally, the influences of the axial compressive load ratio on the new shear wall were investigated.

2. Description of new replaceable component

A typical RC shear wall installed with replaceable components at the two bottom corners is shown in Fig.1. In order to complement the lateral stiffness and shear strength of the RC shear wall and prevent the non-replaceable zone from the damage, the steel plate is embedded at the bottom part of the shear wall.

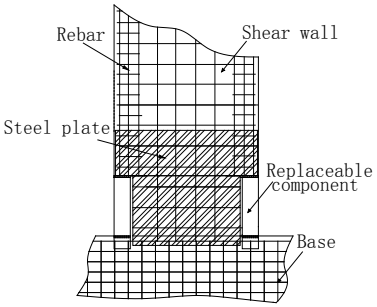

Fig. 1 – RC shear wall with replaceable components at two bottom corners

The constitution of the new replaceable component is shown in Fig.2. The replaceable part, which is located between the top and bottom connection plate, is comprised of the buckling-restrained mild steel core and the concrete filled steel tube (CFST). In order to relieve the bonding between the steel core and the concrete, the surface of the steel core is coated with the plastic film. The two ends of the steel core are strengthened by installing the stiffening rib to prevent them from local failure. When the replaceable component is subjected to the tension, the inner mild steel core will be stretched alone, and the concrete surrounding the steel core does not come into play. When it is compressed, the bulking of the inner mild steel core will be restrained due to the constraint of the surrounding concrete because the core steel is subjected to compression together with the concrete.

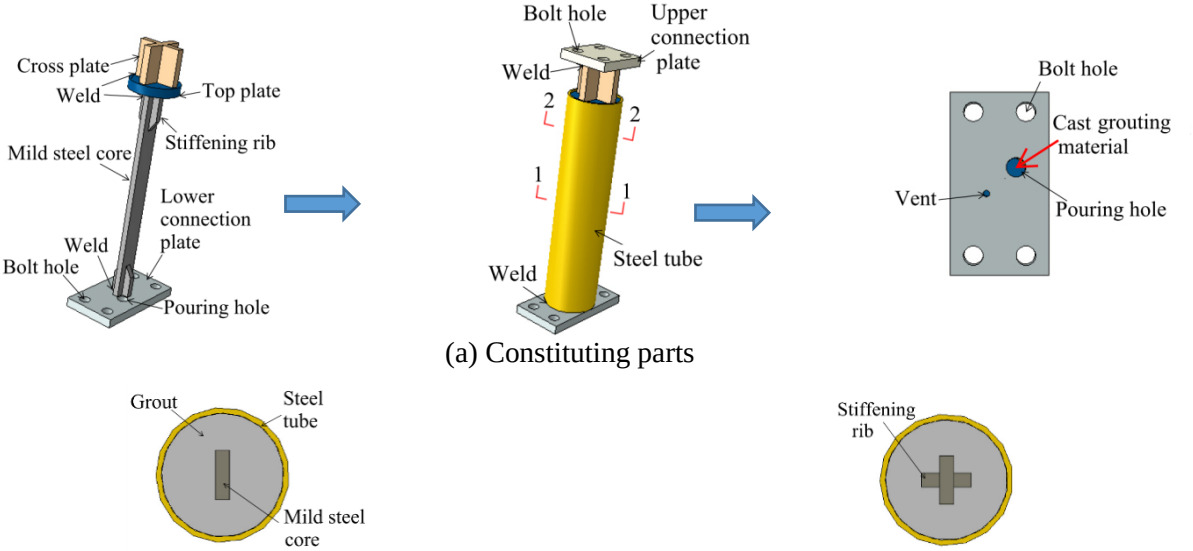

(a) Constituting parts

(b) Section 1-1

(c) Section 2-2

Fig. 2 – Replaceable component

3. Static tests under cyclic loading

3.1 Test specimens

One traditional RC shear wall named CT and two new shear walls named NEW1 and NEW2 installed with the replaceable components at the two bottom corners were designed. All the dimensions of the specimens are identical. The dimensions and steel reinforcement of the specimens are shown in Fig.3. The cross-section length and thickness are 1200mm and 140mm, respectively. The only difference between the two new shear walls is the replaceable component. The parameters of the replaceable components are listed in Table 1.

Table 1 – Parameters of replaceable components

Specimen number	Inner core				CFST		
	Total length /(mm)	Length of stiffening segment/(mm)	Length of yielding segment /(mm)	Cross-sectional area of yielding segment/(mm^2)	Cross-sectional area /(mm^2)	External Diameter of steel pipe/(mm)	Thickness of steel pipe /(mm)
NEW1	500	130	370	640	7527	114	6
NEW2	500	130	370	560	5801	102	6

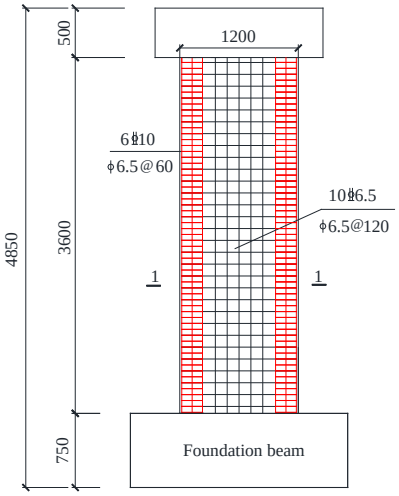

(a) Traditional RC shear wall

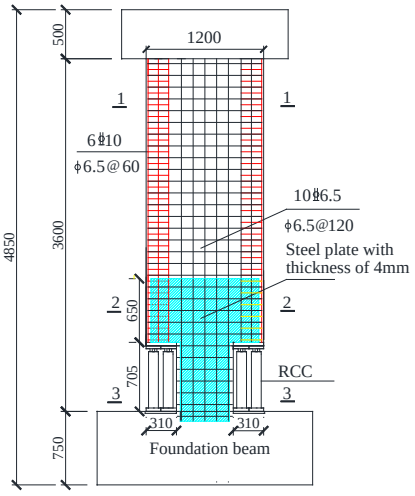

(b) New shear wall installed with the replaceable components

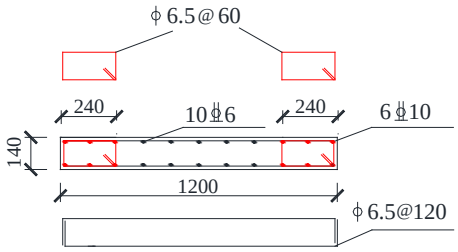

(c) Section 1-1 of CT

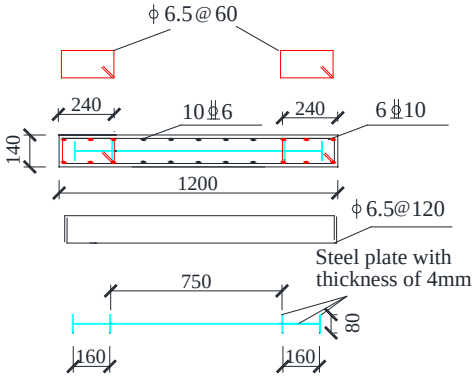

(d) Section 2-2 of new shear walls

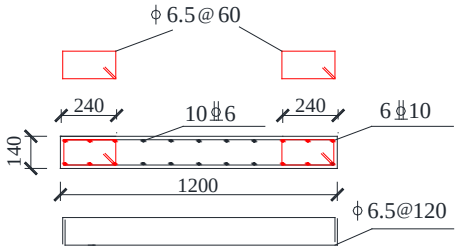

(e) Section 1-1 of new shear walls

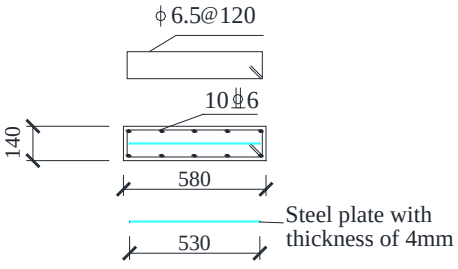

(f) Section 3-3 of new shear walls

Fig. 3 – Constructional details

3.2 Test procedure

First, a vertical load was exerted on the top of specimens by hydraulic jacks and kept approximately constant throughout the entire testing process. The axial compression load ratio for all specimens is 0.25. Prior to cracking of the concrete in the specimens, the horizontal loading was controlled by the force with one cycle at individual force amplitude. After cracking, the lateral load was applied by displacement control with three cycles at individual displacement amplitude. Throughout all test processes, the lateral displacement, force, and the steel strains were recorded electronically. The test setup is shown in Fig.4.

Fig. 4 – Test setup

3.3 Failure mode

As the specimen CT is concerned, the initial damage occurred in the form of horizontal cracks appearing at the bottom of the boundary element. Subsequently, the initial yielding of the longitudinal reinforcement in the boundary element near the pedestal was indicated by the measured strain. Then the diagonal cracks on the web were observed immediately. With the increase in the displacement amplitude, new horizontal and diagonal cracks formed, and the maximum crack width as well as the maximum residual crack width increased. The initial crushing and then spalling of the concrete cover at the bottom of the boundary element was detected. The spalling of the concrete cover extended from the edges of the wall to the web during the later loading. After the concrete cover at the bottom edge completely spalled off and the stirrup and longitudinal reinforcement were exposed, the onset of longitudinal bar buckling at the bottom of the boundary element was observed during subsequent loading cycles. The longitudinal bars fractured after buckling.

The sequences of observed damage were similar for the two new shear wall specimens. The behavior of the specimens was flexure-dominant. The development of damage was as follows: cracking of the concrete at the bottom edge of the inner web wall, tensile yielding of the inner steel core in the replaceable component, tensile yielding of the longitudinal reinforcement at the bottom edge of the web wall, tensile yielding of the steel plate, tensile yielding of the outer steel tube in the circumferential direction, at the bottom edge concrete crushing and spalling, buckling and then fracture of the longitudinal reinforcement, and the fracture of the inner steel core in the replaceable component. It was confirmed that the yielding of the replaceable component occurred before the yielding of the bottom edge of the wall.

Figs.5 and 6 show the damage in the three specimens at the stage with the top drift ratio of 1/100 and 1/50, respectively. It can be found that compared with the traditional shear wall, in the new shear walls the occurring of damage in the main part of the wall was postponed, and the damage was reduced significantly.

(a) CT (b) NEW1 (c) NEW2

Fig. 5 – Damage in the specimens at stage with top drift ratio of 1/100



(a) CT (b) NEW1 (c) NEW2

Fig. 6 – Damage in the specimens at stage with top drift ratio of 1/50

3.4 Lateral force-top displacement relationship

The lateral force-top displacement hysteretic curves for specimens are shown in Fig.7. Compared with CT, the hysteretic behavior of NEW1 and NEW2 is more stable, with less strength and stiffness degradation after the peak load. The skeleton curves are shown in Fig.8. The results derived from the hysteretic curves and skeleton curves are listed in Table 2. The carrying capacity of NEW1 and NEW 2 is 35% and 29% on average in two directions, respectively, higher than that of CT. The displacement ductility factor of NEW1 and NEW2 is 80% and 92% on average in two directions, respectively, higher than that of CT. The total energy of NEW1 and NEW 2 dissipated until ultimate limit state is 3.71 and 3.69 times, respectively, of that of CT. NEW1 with larger cross-sectional area of replaceable components has a little bit higher carrying capacity, lower ductility, and larger dissipated energy than NEW2. In addition, the lateral stiffness of the new shear wall is a little bit higher than that of the traditional shear wall.

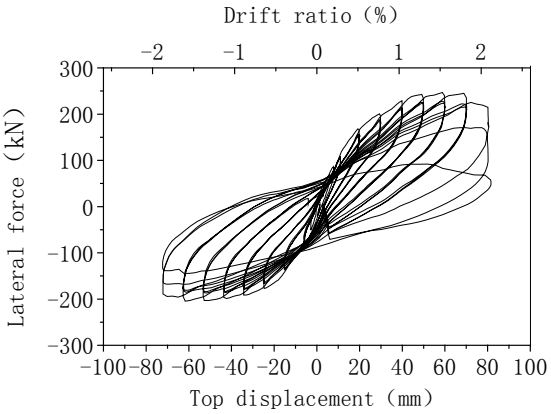

(a) CT

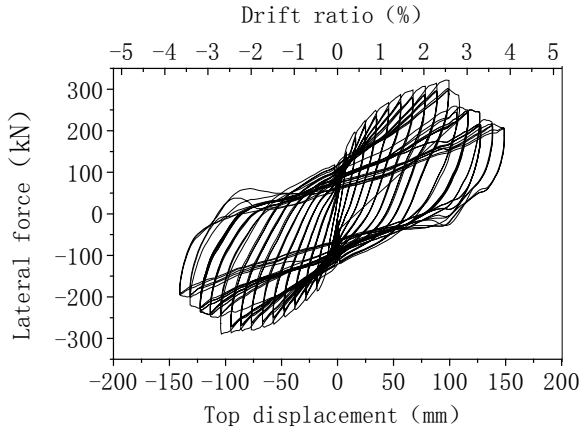

(b) NEW1

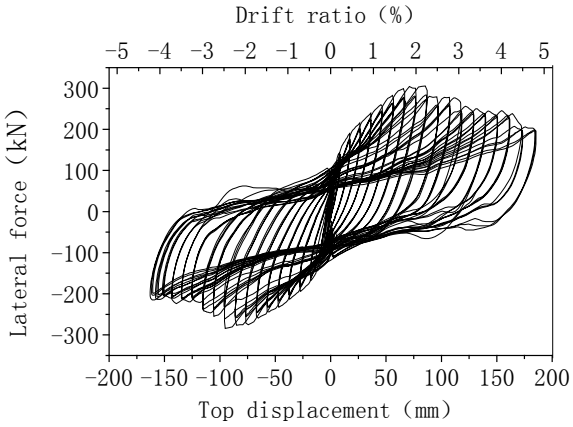

(c) NEW2

Fig. 7 – Lateral force-top displacement hysteretic curves

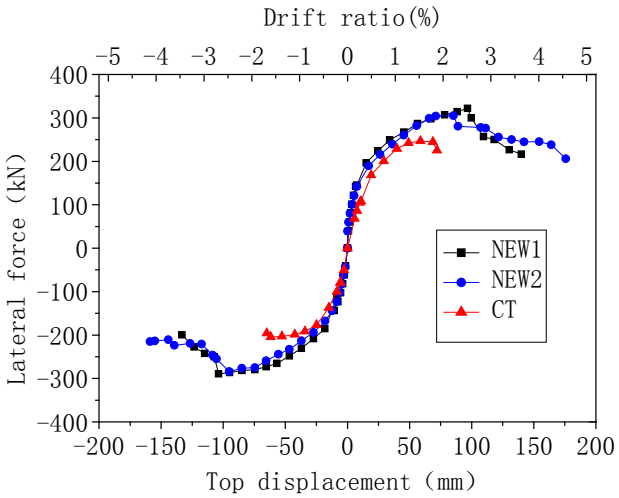

Fig. 8 – Comparison of lateral force-top displacement skeleton curves

Table 2 – Summary of experimental results

Specimen number	Yield displacement(mm)		Peak load(kN)		Ultimate displacement(mm)		Ductility factor		Energy dissipation until ultimate limit state (kN·m)
	Positive	Negative	Positive	Negative	Positive	Negative	Positive	Negative	
CT	21.2	14.8	246.9	204.5	80.1	70.2	3.78	4.74	197.17
NEW1	13.3	15	321.9	286.2	105.7	111.5	7.96	7.40	731.31
NEW2	13.8	14.7	305.3	276.6	119.9	112.4	8.66	7.66	727.14

4. Finite element analysis

4.1 Analytical model

The finite element models for the two types of shear wall specimens as shown in Fig.9 were established by using the commercial software ABAQUAS. The steel rebars were simulated by the space truss element T3D2. The concrete, the steel tube, the steel plate, and the steel core were simulated by linear reduced integration three-dimensional solid element C3D8R. Let Y direction be the axial direction of replaceable components, then the inner steel core and the concrete are coupled at the X and Z direction to simulate the CFT constraint effects on the inner core, while the DOF in Y direction is released to simulate the relative displacement between the inner core and the CFT.

The plasticity damage model based on continuum damage mechanics was adopted to describe the nonlinear behavior of the concrete. In this model two damage patterns, tensile cracking and compressive crushing, are considered. Tensile damage factor d_t and compressive damage factor d_c are used to measure the damage level of two damage patterns and decrease the stiffness accordingly. The Mander model [14] was used to describe the stress-strain behavior of the concrete. The damage factor can be expressed by the following equations [15]:

$$d_t = 1 - \frac{\sigma_t E_c^{-1}}{\varepsilon_t^{pl}(1/b_t - 1) + \sigma_t E_c^{-1}} \tag{1}$$

$$d_c = 1 - \frac{\sigma_c E_c^{-1}}{\varepsilon_c^{pl}(1/b_c - 1) + \sigma_c E_c^{-1}} \tag{2}$$

where subscript c and t represent compression and tension, respectively, b_t=0.9, b_c=0.7, and ε_c^{pl} and ε_t^{pl} are the plastic compression strain and the tension strain, respectively. The mechanical properties of steel were defined by the kinematic and isotropic combined model in ABAQUS. The bilinear relationship models the uniaxial stress-strain behaviour of the steel. It is characterised by the modulus of elasticity, the yield strength and the post-yield stiffness.

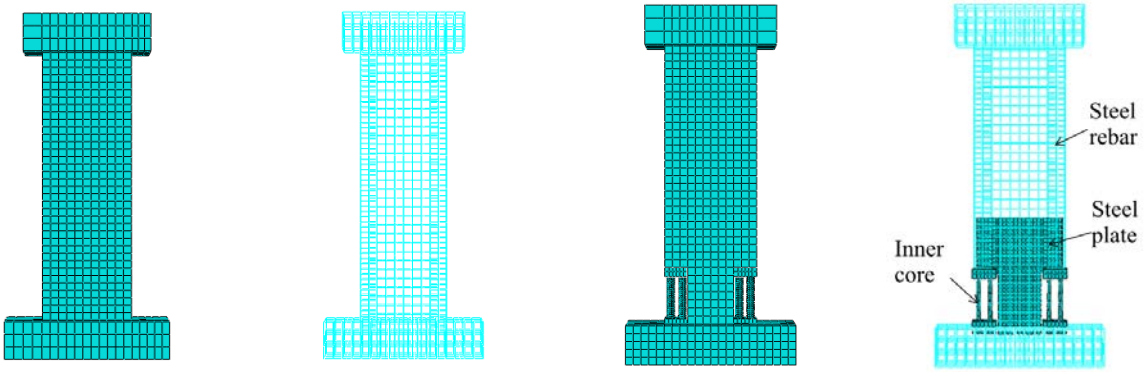

(a) Traditional shear wall (b) Steel rebars in traditional shear wall (c) New shear wall (d) Steel in new shear wall

Fig. 9 – Finite element models

4.2 Analytical results

The pushover analysis was carried out for the three specimens. The comparison of calculated lateral force-top displacement skeleton curves with test results is shown in Fig.10. The analytical results agree well with the test results. The vertical plastic strain responses of the specimens at the stage with the top drift ratio of 2% are shown in Fig.11. The strain responses roughly agree with the damage of the specimens shown in Fig.6.

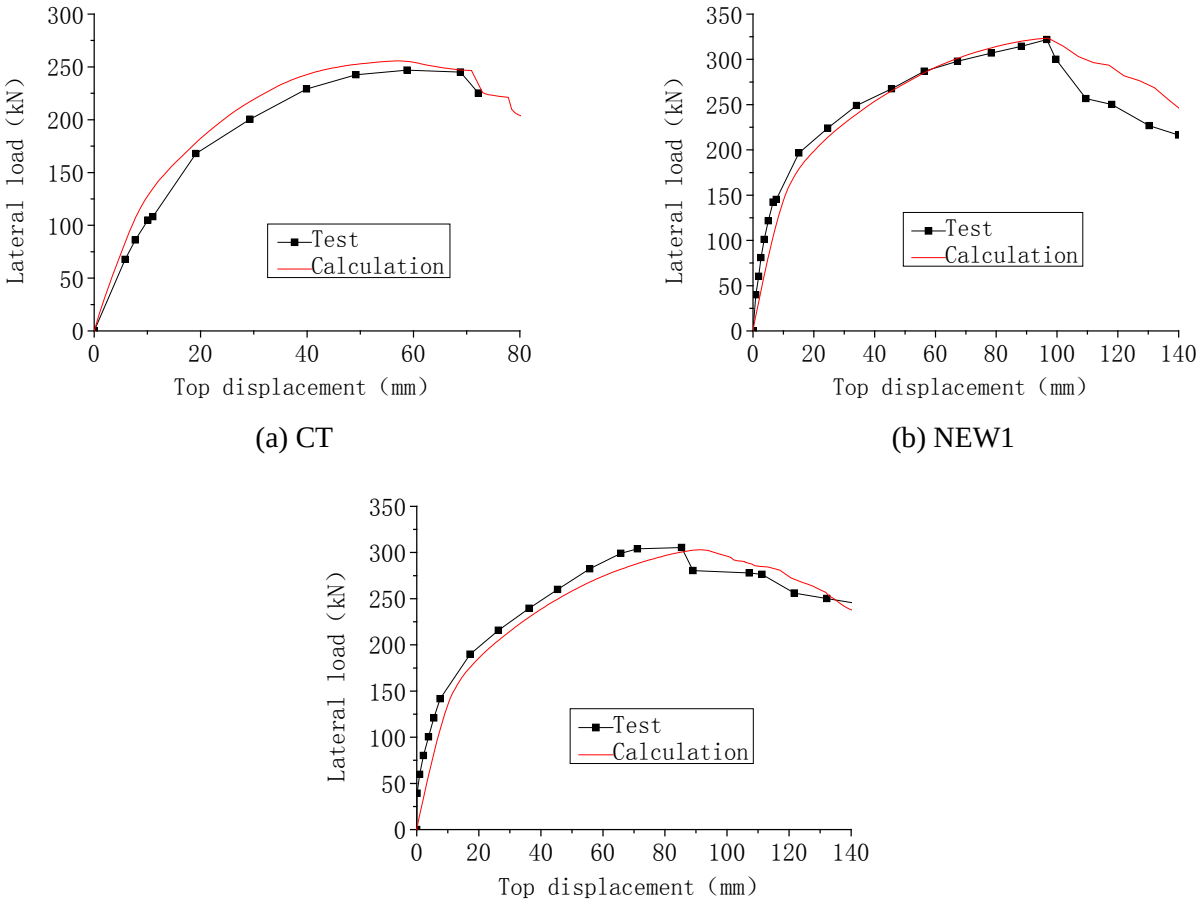

(a) CT (b) NEW1

(c) NEW2

Fig. 10 – Comparison of lateral force-top displacement skeleton curves

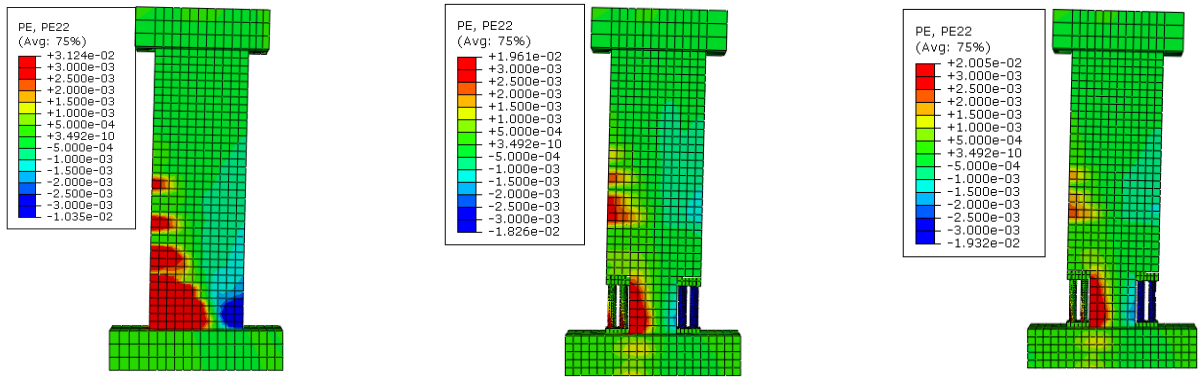

(a) CT (b) NEW1 (c) NEW2

Fig. 11 – Plastic strain component at the stage with the top drift ratio of 2%

In the real case the axial compressive load ratio of the shear wall in tall buildings could be higher that the specimens in this test. Therefore, the performance of the specimens with the axial compressive load ratio of 0.4 and 0.6 was studied by using the above verified analytical models in addition. The vertical plastic strain responses of the specimens at the stage with the top drift ratio of 1.5% are shown in Fig.12. It can be found that as expected, the compressive damage of the new shear wall concentrates on the replaceable component while the left part keeps almost intact, the tensile strain of the new shear wall is also much lower than the traditional shear wall.

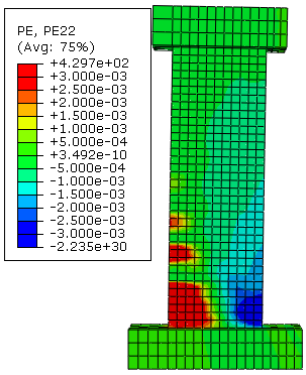

(a) CT with axial compressive load ratio of 0.4

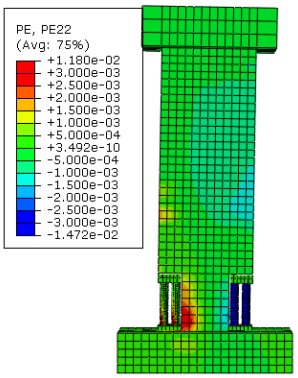

(b) NEW1 with axial compressive load ratio of 0.4

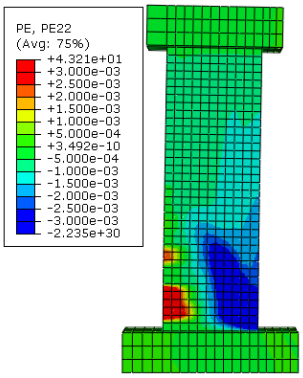

(a) CT with axial compressive load ratio of 0.6

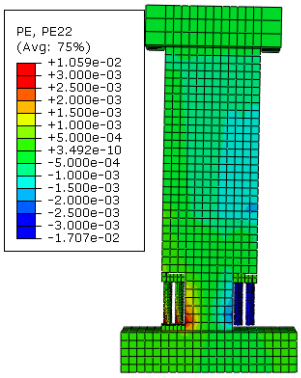

(b) NEW1 with axial compressive load ratio of 0.6

Fig. 12 – Plastic strain component at the stage with the top drift ratio of 1.5%

The comparison of the lateral load-top displacement skeleton curve is shown in Fig.13. It is indicated that in the case under higher compressive loading similarly the carrying capacity and deformation capacity of the new shear wall are much higher than that of the traditional shear wall.

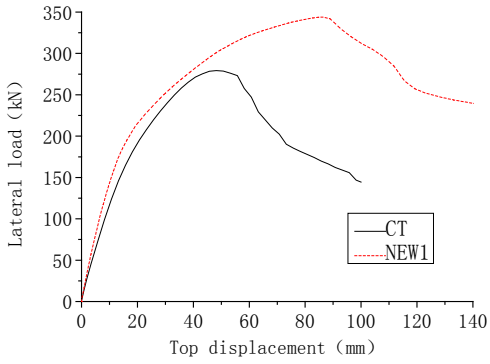

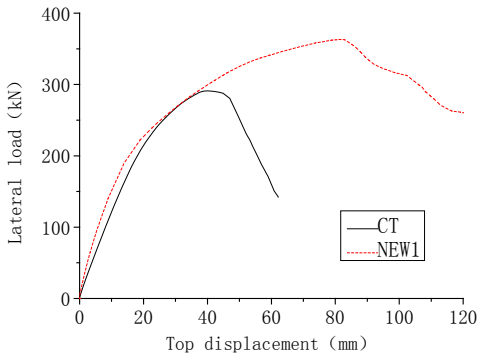

(a) Specimens with axial compressive load ratio of 0.4 (b) Specimens with axial compressive load ratio of 0.6

Fig. 13 – Lateral load-top displacement skeleton curve

4. Conclusions

An earthquake resilient RC shear wall installed with a new kind of replaceable component at the two bottom corners was proposed in this study. The constructional details of the replaceable component was introduced. The improved seismic performance of the new shear wall was verified by the quasi-static tests carried out on the new shear wall. The analytical models for the two types of shear walls were developed with the aid of the commercial

software ABAQUAS and verified by the test results. The test and finite element analysis results show that the new earthquake resilient RC shear wall has much higher ductility and strength than the traditional RC shear wall. Compared with the shear wall with replaceable rubber bearings, the new shear wall proposed in this study has larger lateral strength and stiffness, and the remaining part excluding the replaceable components is better protected when subjected to the strong earthquake.

Acknowledgements

The authors are grateful for the support from the Ministry of Science and Technology of China through Grant No. SLDRCE14-B-2 and National Natural Science Foundation of China under grant No. 51478354.

References

[1] Hitaka T, Sakino K (2008): Cyclic tests on a hybrid coupled wall utilizing a rocking mechanism. *Earthquake Engineering and Structural Dynamics*, **37** (14), 1657-1676.

[2] Wada A, Qu Z, Ito H, Motoyui S, Sakata H, Kasai K (2009): Seismic retrofit using rocking walls and steel dampers. *Proceedings of ATC/SEI Conference on Improving the Seismic Performance of Existing Buildings*, San Francisco. CA, USA: Applied Technology Council.

[3] Restrepo JI, Rahman A (2007): Seismic performance of self-centering structural walls incorporating energy dissipaters. *Journal of Structural Engineering*, **133** (11), 1560-1570.

[4] Smith BJ, Kurama YC, McGinnis MJ (2013): Behavior of precast concrete shear walls for seismic regions: comparison of hybrid and emulative specimens. *Journal of Structural Engineering*, **139** (11), 1917-1927.

[5] Ozaki F, Kawai Y, Tanaka H, Okada T, Kanno R (2010): Innovative damage control systems using replaceable energy dissipating steel fuses for cold-formed steel structures. *Proceedings of The 20th International Specialty Conference on Cold-formed Steel Structures-Recent Research and Developments in Cold-Formed Steel Design and Construction*, University of Missouri-rolla, 443-457.

[6] Ozaki F, Kawai Y, Kanno R, Hanya K (2013): Damage-control systems using replaceable energy-dissipating steel fuses for cold-formed steel structures: seismic behavior by shake table tests. *Journal of Structural Engineering*, ASCE, **139** (5), 787-795.

[7] Hitaka T, Sakino K (2008): Cyclic tests on a hybrid coupled wall utilizing a rocking mechanism. *Earthquake Engineering and Structural Dynamics*, **37** (14), 1657-1676.

[8] Kurama Y, Sause R, Pessiki S, Lu LW (1999): Lateral load behavior and seismic design of unbonded post-tensioned precast concrete walls. *ACI Structural Journal*, **96** (4), 622-633.

[9] Wada A, Qu Z, Ito H, Motoyui S, Sakata H, Kasai K (2009): Seismic retrofit using rocking walls and steel dampers. Proceedings of ATC/SEI *Conference on Improving the Seismic Performance of Existing Buildings and Other Structures*. San Francisco. CA, USA: Applied Technology Council.

[10] Panian L, Steyer M, Tipping S (2007): Post-Tensioned concrete walls for seismic resistance. PTI Journal, **5** (1), 7-12.

[11] Kurama Y C, Brad D, and Qiang S (2006): Experimental Evaluation of Posttensioned Hybrid Coupled Wall Subassemblages. Journal of Structural Engineering, **132** (7), 1017-1029.

[12] Lyons RM, Christopoulos C, and Montgomery MS (2012): Enhancing the seismic performance of RC coupled wall high-rise buildings with viscoelastic coupling dampers. Proceedings of 15WCEE, September 24-28, Lisbon, Portugal, Paper ID: 1573.

[13] Lu XL, Mao YJ, Chen Y, Liu JJ, Zhou Y (2013): New structural system for earthquake resilient design. Journal of Earthquake and Tsunami, **7** (3).

[14] Mander JB, Priestley MJN, Park R. (1988): Theoretical stress–strain model for confined concrete. *Journal of Structural Engineering*, **114**(8), 1804-1826.

[15] Birtel V, Mark P (2006): Parameterized Finite Element Modeling of RC Beam Shear Failure. 2006 ABAQUS User's Conference, Taiwan, 95-108.